

## INVESTIGATING THE SURFACE OF TITAN IN THE 1-2.8 $\mu\text{m}$ RANGE WITH CASSINI/VIMS HYPERSPECTRAL IMAGES

S. Le Mouélic<sup>1</sup>, T. Cornet<sup>1</sup>, S. Rodriguez<sup>2</sup>, C. Sotin<sup>1,5</sup>, J. W. Barnes<sup>3</sup>, R.H. Brown<sup>4</sup>, K.H. Baines<sup>5</sup>, B.J. Buratti<sup>5</sup>, R.N. Clark<sup>6</sup>, Axel Lefèvre<sup>1</sup>, P.D. Nicholson<sup>7</sup>. <sup>1</sup>Laboratoire de Planétologie et Géodynamique, Nantes, France, <sup>2</sup> Laboratoire AIM, CEA, Gif/Yvette, France, <sup>3</sup>University of Idaho, USA, <sup>4</sup>Lunar and Planetary Lab and Stewart Observatory, University of Arizona, Tucson, <sup>5</sup>JPL, Pasadena, USA. <sup>6</sup>USGS Denver. <sup>7</sup>Cornell University, Astronomy Department, USA. [stephane.lemouelic(at)univ-nantes.fr]

**Introduction:** Titan is veiled by a dense atmosphere which absorbs and scatters both the incoming solar flux and the signal reflected by the surface. The surface can still be seen at specific wavelengths at 1.08, 1.27, 1.59, 2.03, 2.69-2.78 and 5  $\mu\text{m}$ , where the atmospheric gases are the most weakly absorbing [1,2]. We focus in this paper on the global mapping of Titan's surface at these wavelengths using the Visual and Infrared Mapping Spectrometer (VIMS) onboard Cassini, with the objective to reduce the atmospheric contribution in the short wavelengths surface windows.

**Methodology:** We have computed a global hyperspectral mosaic of all VIMS data taken during the nominal and equinox Cassini mission (from Ta in October 2004 to T70 in June 2010) (Figure 1). Coarse resolution images are used as background, and progressively finer resolutions are put on top. A series of filters has been designed to remove pixels acquired with extreme viewing geometries, which produce strong atmospheric artifacts.

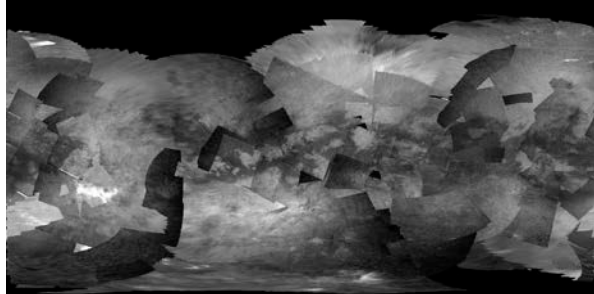


Figure 1: Global mosaic of VIMS data at 5  $\mu\text{m}$  acquired between Ta and T70.

At first order, the spectral radiance or intensity  $I(\lambda, \phi)$  in  $\text{W}/\text{m}^2/\mu\text{m}/\text{sr}$  measured by the instruments can be summarized by the following simplified radiative transfer equation [3]:

$$I(\lambda, \phi) = F(\lambda) \cdot \cos(i) \cdot R(\lambda) \cdot \exp(-\tau) + I_{\text{scat}}(\lambda, \phi)$$

where  $\lambda$  is the wavelength,  $\phi$  is the phase angle,  $F$  is the solar radiance (in  $\text{W}/\text{m}^2/\mu\text{m}/\text{sr}$ ),  $i$  is the incidence angle,  $R$  is the bidirectional reflectance of a perfect Lambertian surface,  $\tau$  is the optical depth of the atmosphere, and  $I_{\text{scat}}$  an additive term that includes the light scattered by the atmosphere. According to this formalism,  $I/F$  in the surface windows should be directly correlated to  $\cos(i)$  in areas of homogeneous reflectance values, provided that

we can get rid of the  $I_{\text{scat}}$  term. This  $I_{\text{scat}}$  term can be neglected at first order in the 5  $\mu\text{m}$  window [4,5]. For shorter wavelengths, we use an average of the left and right band wings, respectively corresponding to the first wavelengths at the shortward and longward side respectively of a spectral window where the surface cannot be seen, as a proxy for  $I_{\text{scat}}$ . These wavelengths probe almost all the column of atmosphere, except the very last layers close to the ground. They therefore contain almost all the additive scattering contribution provided by the atmosphere. To account for the difference with the exact amount of additive term in the center of the atmospheric surface window, where the methane is the most transparent, we empirically multiply this contribution by a scaling factor  $k$ . This process is illustrated for the 1.27  $\mu\text{m}$  window in the scatter plots shown in Figure 2. The plot is restricted to the area indicated by the red rectangle, which corresponds to homogeneously bright materials only.

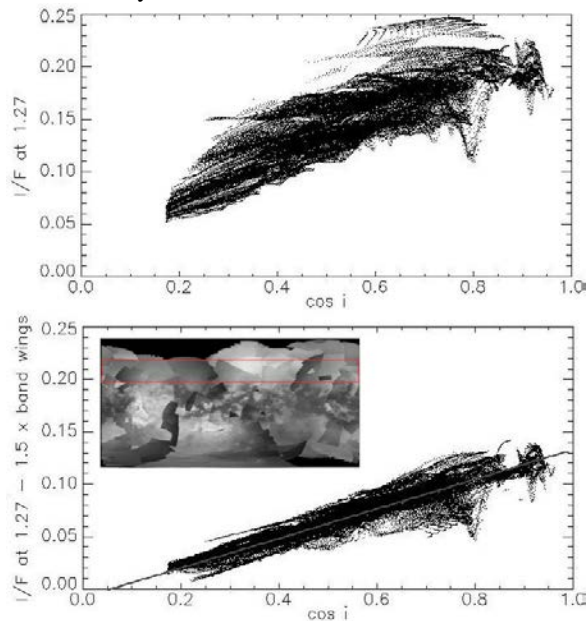


Figure 2 : 2-D scatter plots of  $I/F$  at 1.27  $\mu\text{m}$  versus  $\cos(i)$ . Top: without any correction. Bottom : after the optimized subtraction of the scaled band wings.

After this empirical correction process of the additive term, the division by  $\cos i$  can be used to normalize at first order the viewing geometry in the corresponding image (Figure 3).

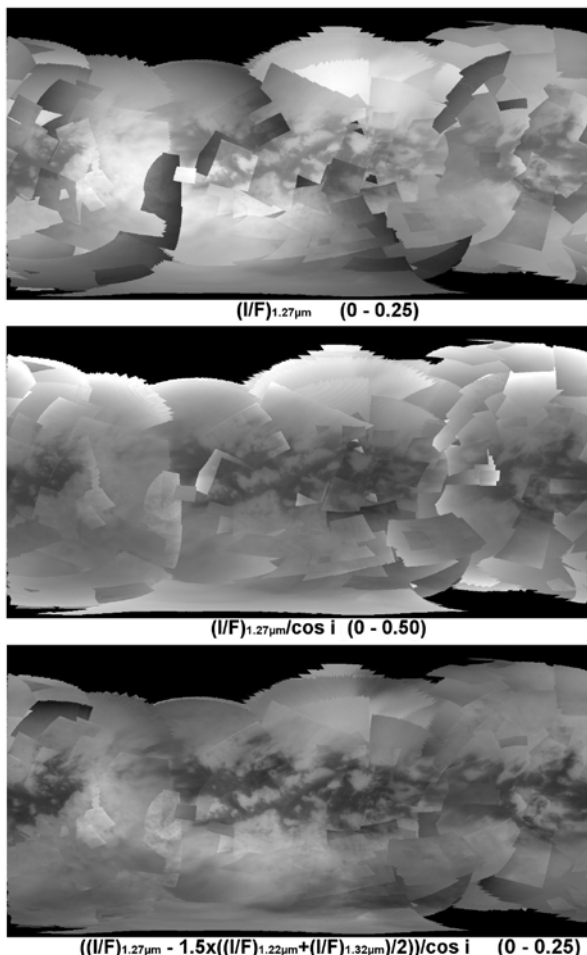


Figure 3 : global mosaic of Titan at 1.27  $\mu\text{m}$ . Top : raw I/F values. Middle: same map after division by cosine of the incidence angle. Bottom: empirical subtraction of the additive scattering contribution and division by  $\cos(i)$ . The maps are displayed in black and white with a linear stretch corresponding to the values indicated in parenthesis.

The main discrepancies which are still present between individual images in this global mosaic integrating seven years of observations are due to transient phenomenon such as clouds, residual calibration artifacts and second order photometric effects.

**Conclusion and Perspectives :** The global mapping of the surface of Titan free of atmospheric and photometric effects is still a challenging task. We have presented an empirical approach that can be used in order to improve the quality of the maps and correct the images at a first order. This can be useful to provide a comparison with other independent analyses based either on alternative empirical approaches, or on complete radiative transfer modeling, paving the way for further refined algorithms. Further refinement could

for example include the use of the semi-automated cloud detection technique of [6], or a refined surface photometric function [7].

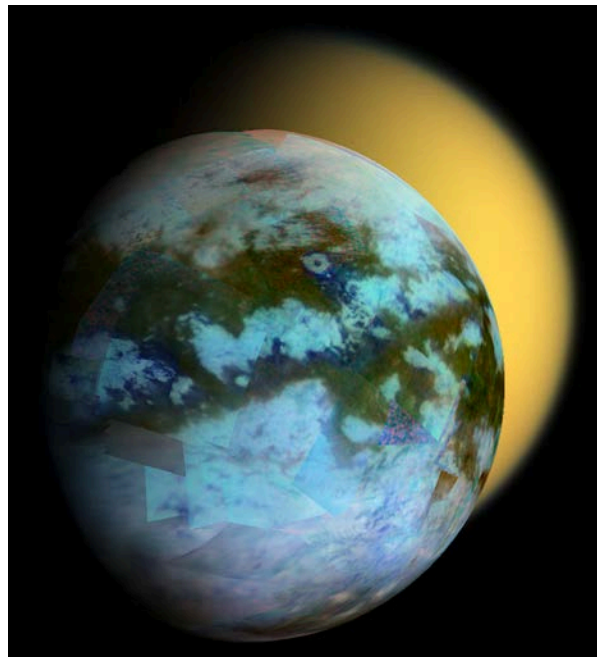


Figure 4 : Global views of Titan from the Cassini spacecraft. The foreground image is a false-color composite of the global corrected VIMS mosaic of Titan with Red=5.0  $\mu\text{m}$ , G=2.0  $\mu\text{m}$ , B=1.27  $\mu\text{m}$ . The background is an ISS true-color image.

**Bibliography :** [1] Brown R.H. et al., The Cassini Visual and Infrared Mapping Spectrometer investigation, *Space Sci. Rev.*, 115, pp. 111–168, 2004. [2] Sotin et al., Release of volatiles from a possible cryovolcano from near-infrared imaging of Titan, *Nature*, 435, pp.786-789, 2005. [3] Sotin et al., Observations of titan's northern lakes at 5 microns: Implications for the organic cycle and geology, submitted to *Icarus*. [4] Le Mouélic et al., Photometric properties of Titan's surface at 5  $\mu\text{m}$  investigated with Cassini/VIMS hyperspectral images 42<sup>nd</sup> LPSC, 1608, p.1495,2011. [5] Rodriguez et al., Cassini/VIMS observations of the Huygens landing site on Titan, *Planet. Space Sci.*, 54, pp 1510-1523, 2006. [6] Rodriguez S. et al., Global circulation as the main source of cloud activity on Titan, *Nature*, 459, 678-682, 2009. [7] Schröder and Keller, The unusual phase curve of Titan's surface observed by Huygens' Descent Imager/Spectral Radiometer, *Planet. Space Sci.*, 57, p1963-1974, 2009.